J Mater Sci (2011) 46:1405–1413
DOI 10.1007/s10853-010-4934-1

Phase equilibria and thermodynamic modeling in the Ge–Zr binary system

Chunsheng Sha · Liangcai Zhou · Shuhong Liu · Yong Du · Tie Gang · Honghui Xu

Received: 8 July 2010 / Accepted: 16 September 2010 / Published online: 6 October 2010

Abstract The Ge–Zr system is assessed by means of calculation of phase diagram (CALPHAD) approach, supplemented with decisive experiments and enthalpies of formation computed via Vienna ab initio simulation package (VASP) code. Nine Ge–Zr alloys were prepared by arc melting the pure elements. The annealed samples were analyzed by means of XRD, optical microscopy, and SEM/EDX. Five compounds are observed in the equilibrium condition. The enthalpies of formation for Zr_5Ge_3, Zr_5Ge_4, and $ZrGe_2$ are computed via first-principles calculations. These enthalpies of formation are used as key "experimental data" in the CALPHAD approach in order to obtain the thermodynamic parameters with sound physical meaning. A consistent thermodynamic data set for the Ge–Zr system is finally obtained based on the present work and the literature data. Comparisons between the calculated and measured phase diagram and thermodynamic quantities show that the accurate experimental information is satisfactorily accounted for by the present thermodynamic description.

C. Sha · L. Zhou · S. Liu · Y. Du (✉) · H. Xu
Science Center for Phase Diagram and Materials Design and Manufacture, Central South University, Changsha 410083, Hunan, People's Republic of China
e-mail: yong-du@mail.csu.edu.cn

C. Sha · L. Zhou · S. Liu · Y. Du · H. Xu
Research Institute of Powder Metallurgy, Central South University, Changsha 410083, Hunan, People's Republic of China

T. Gang
State Key Laboratory of Advanced Welding Production Technology, Harbin Institute of Technology, Harbin 150001, China

Introduction

Zirconium alloys are widely used in many fields of modern technology, such as the production of special steels, electrical engineering, nuclear power, etc. Interaction between zirconium and germanium results in the formation of intermetallic compounds with good fabrication properties, such as high-hardness and corrosion resistance [1]. The design and development of high quality Ge–Zr materials need information about the phase equilibria and thermodynamic properties of the Ge–Zr system.

No thermodynamic assessment of the Ge–Zr system has been reported in the literature. A thorough assessment of the Ge–Zr system is necessary in order to provide a reliable set of thermodynamic parameters for thermodynamic extrapolations to related ternary systems. The present work is devoted to obtain an optimized data set for the Ge–Zr system via a combined approach of CALPHAD, experiments and ab initio calculations for enthalpy of formation.

Evaluation of experimental data

This system has been previously evaluated by Abriata et al. [2]. The Ge–Zr system contains five intermetallic compounds (Zr_3Ge, Zr_5Ge_3, Zr_5Ge_4, ZrGe, and $ZrGe_2$). Several groups of authors [1, 3–6] have contributed to the identification of the compounds in the Ge–Zr system. Their recommended crystal structure and stoichiometries are accepted in the present modeling. The crystal structural data of Ge–Zr compounds are listed in Table 1.

Table 1 Crystal structure and lattice parameters of the compounds in the Ge–Zr system

Phase	Structure type	Pearson symbol	Space group	Lattice parameters (nm)	Reference
Zr_3Ge	Ti_3P	*tP*32	$P4_2/n$	$a = 1.108$, $c = 0.548$	[1]
Zr_5Ge_3	Mn_5Si_3	*hP*16	$P6_3/mcm$	$a = 0.7993$, $c = 0.5594$	[1]
Zr_5Ge_4	Zr_5Si_4	*tP*36	$P4_12_12$	$a = 0.7238$, $c = 1.3154$	[1]
ZrGe	FeB	*oP*8	*Pnma*	$a = 0.7068$, $b = 0.3904$, $c = 0.5396$	[1]
$ZrGe_2$	$ZrSi_2$	*oC*12	*Cmcm*	$a = 0.3789$, $b = 1.4975$, c = 0.3761	[1]

In this section, all of the experimental phase diagram and thermodynamic data available for the Ge–Zr system are briefly evaluated. Table 2 presents the phase diagram and thermodynamic data, which are considered in the present thermodynamic modeling.

Table 2 Summary of the literature data included in the optimization

Type of data	Experimental technique	Reference
Solubility of Ge in (Zr)	XRD and MA	[3]
Solubility of Zr in Ge	XRD and MA	[3]
Cooling curve arrest	DTA	[3]
Liquid phase	MA, incipient melting, and DTA	[3]
The enthalpies of mixing	High-temperature calorimetry	[10]
Zr_3Ge phase	XRD and MA	[2]
Crystal structure	XRD	[1]
Zr_5Ge_3 phase	XRD and MA	[3]
	XRD and EDX	This work
Enthalpy of formation	High-temperature calorimetry	[11]
	Ab initio calculation	This work
Zr_5Ge_4 phase	XRD	[1]
	XRD and EPMA	[8]
	XRD and EDX	This work
Enthalpy of formation	Ab initio calculation	[21]
	Ab initio calculation	This work
ZrGe phase	XRD and MA	[3]
	XRD and EDX	This work
$ZrGe_2$ phase	XRD and MA	[3]
	XRD and EDX	This work
Enthalpy of formation	Ab initio calculation	This work
Congruent temperature	Incipient melting	[3]
Eutectic temperature	Incipient melting, DTA, and optical pyrometry	[3]
Peritectic temperature	Incipient melting and optical pyrometry	[3]
Peritectoid temperature	DTA	[3]

Phase diagram data

Carlson et al. [3] was the first to make the phase diagram measurements for the Ge–Zr system, using optical microscopy (OM), X-ray diffraction (XRD), thermal analysis, and melting observations. Four intermediate phases, Zr_3Ge, Zr_5Ge_3, ZrGe, and $ZrGe_2$ were proposed by Carlson et al. [3]. Using XRD method, Rossteutscher and Schubert [4] and Pfeifer and Schubert [5] identified the Zr_5Ge_4 phase as the tetragonal Zr_5Si_4-type structure, when they investigated the samples previously heated to 1620 °C. Seropegin et al. [6] also observed this phase in the ternary system Nb–Zr–Ge at 900 °C. Based on these authors' work, an assessed version of the phase diagram was given by Abriata et al. [2]. However, the region between Zr_5Ge_3 and ZrGe of this assessed phase diagram remains uncertain. Based on the work of Seropegin et al. [6],

Table 3 Summary of identified phase and their compositions for the Ge–Zr alloys annealed at 1123 K for 3 weeks

No.	Comp. (at.%) Nom[a]		Phase analysis XRD	EDX results (at.%)	
	Ge	Zr		Ge	Zr
1#	25.53	74.47	Zr_3Ge	24.5	75.5
			Zr_5Ge_3	37.7	62.3
2#	30.76	69.24	Zr_3Ge	26.5	73.5
			Zr_5Ge_3	37.1	62.9
3#	38.23	61.77	Zr_5Ge_3	38.4	61.6
4#	40.98	59.02	Zr_5Ge_3	40.4	59.6
			Zr_5Ge_4	46.4	53.6
5#	44.61	55.39	Zr_5Ge_4	44.4	55.6
			ZrGe	49.6	50.4
6#	49.10	50.90	Zr_5Ge_4	45.9	54.1
			ZrGe	49.4	50.6
7#	60.23	39.77	ZrGe	50.8	49.2
			$ZrGe_2$	66.4	33.6
8#	66.05	33.95	$ZrGe_2$	66.4	33.6
9#	80.03	19.97	$ZrGe_2$	66.9	30.1
			Ge	99.9	0.1

[a] The nominal sample composition was calculated under the assumption that all weight losses during sample preparation are due to loss of Ge

Rudometkina et al. [1] confirmed that there are five compounds in the Ge–Zr system: Zr_3Ge, Zr_5Ge_3, Zr_5Ge_4, ZrGe, and $ZrGe_2$, and they believed that Zr_5Ge_3 melts with a congruent melting and other intermetallic compounds are formed by peritectic reactions. Recent works by Zatorska et al. [7], Ponweiser et al. [8], and Marker et al. [9] reported that the homogeneity regions of the compounds in the Ge–Zr system are quite narrow except for Zr_5Ge_3, which reaches 2–3 at.% germanium.

Thermodynamic data

By means of a high-temperature isoperibolic calorimeter, the enthalpy of mixing in the liquid phase has been determined at 1700 °C by Beloborodova [10] in the composition range from 0 to 22 at.% Ge. The enthalpy of formation for compound Zr_5Ge_3 was determined by Jung and Kleppa [11] using high-temperature calorimetry. These experimental thermodynamic data are considered to be reliable and thus utilized in the present optimization.

Experimental procedure

All samples were prepared from 99.5% Zr chips and 99.999% Ge pieces (both supplied by Huizhou hi-purity rare earth metal material Co., LTD, China). Calculated amounts of metals were weighed to an accuracy of 0.1 mg and arc melted on a water-cooled copper plate under an argon atmosphere. Each alloy was remelted four times to ensure homogeneity. Because of the relatively high vapor pressure of Ge it was not possible to melt the metals

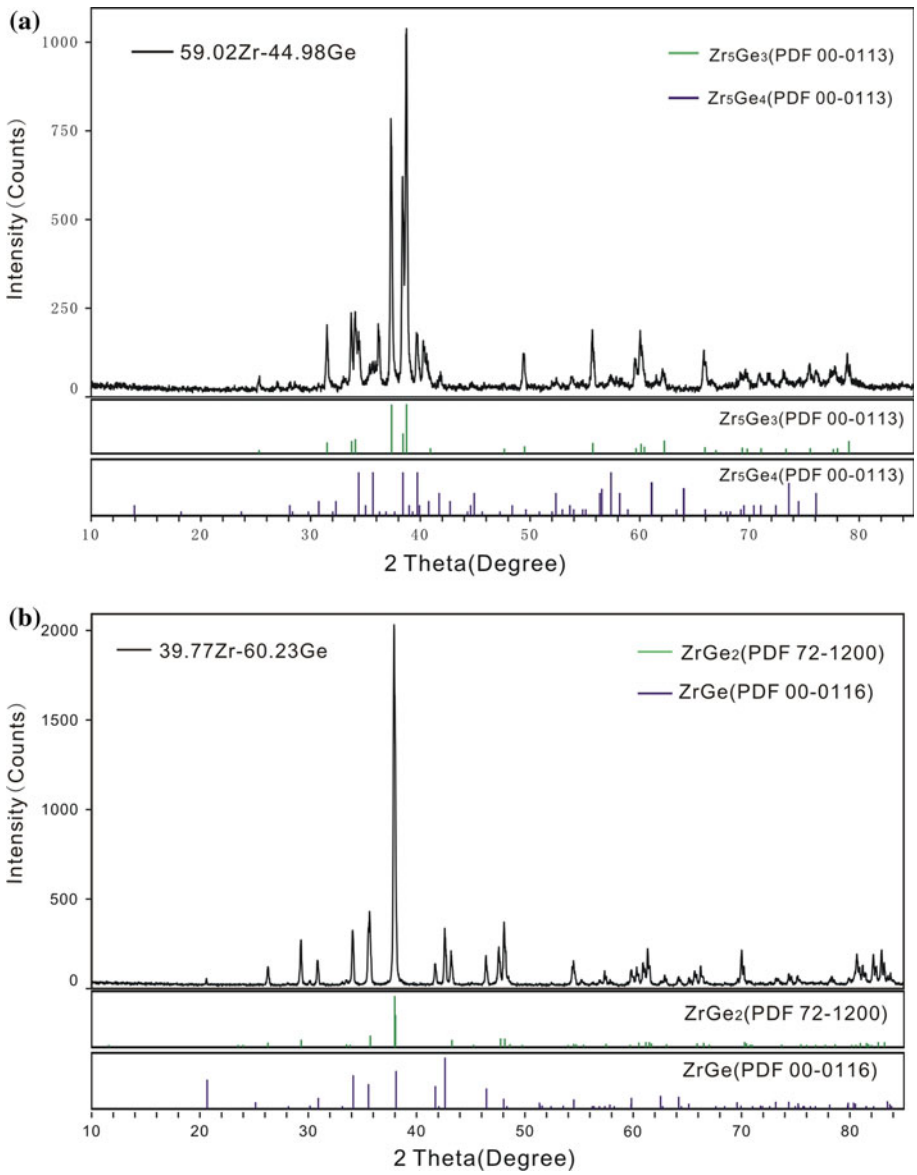

Fig. 1 The XRD patterns of alloy 4# (**a**) and alloy 7# (**b**)

without a considerable mass loss due to evaporisation of Ge. In view of the compensation for this loss, some extra Ge was added before the subsequent melting process. It is assumed that the weight loss during the arc melting is derived only from the loss of Ge. The compositions of the prepared alloys are shown in Table 3. All the alloys prepared by the above procedure were annealed at 1023 K for 3 weeks in an L4514-type diffusion furnace, and then quenched in cold water.

After being quenched by rapidly submersing the capsules in water, the samples were investigated by means of XRD (Rigaku D-max/2550 VB^+, Japan), OM (Leica DMLP, Germany), and SEM/EDX (JSM-6360LV, JEOL, Japan). The phase identification was performed by means of XRD at 40 kV and 300 mA with Cu K_α radiation. Microstructure of the solidified and annealed alloys was observed by OM. The compositions of the phases were measured by SEM/EDX.

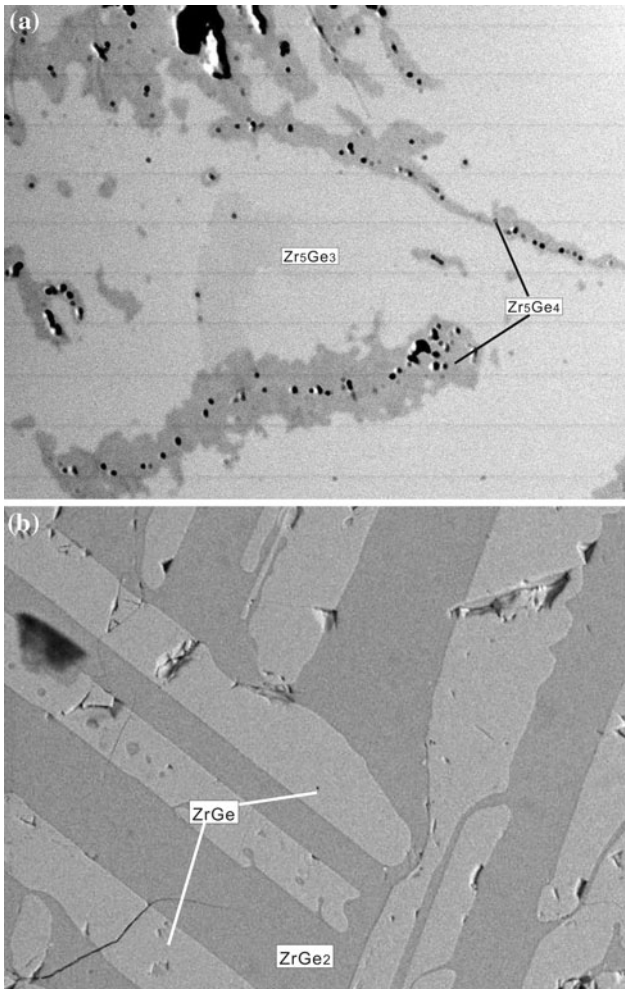

Fig. 2 The backscattered electron image (BEI) of alloy 4# (**a**) and the backscattered electron image of alloy 7# (**b**)

Ab initio calculation for enthalpy of formation

In the present work, first-principles calculation is employed to obtain $\Delta_f H$ for the compounds Zr_5Ge_3, $ZrGe_2$, Zr_5Ge_4. The total energies of the Zr_5Ge_3, $ZrGe_2$, Zr_5Ge_4, Zr, and Ge were calculated by using density functional theory (DFT) [12] within a generalized gradient approximation (GGA) [13] as well with projector augmented-wave (PAW) pseudopotentials [14], as implemented in the Vienna ab initio simulation package (VASP) [15, 16]. The GGA proposed by Perdew, Burke and Ernzerh of (PBE) [17] was used in the calculation. Brillouin zone integrations were performed using a Monkhorst–Pack mesh [18], i.e., 11*11*13 for Zr_5Ge_3 and 9*9*5 for $ZrGe_2$, Zr_5Ge_4. The energy cut off 400 eV was used to converge total energy to less than 1 mev/atom. The structure was fully relaxed using the Methfessel–Paxton smearing method [19] and a final self-consistent static calculation via the tetrahedron smearing method with Blochl corrections [20] was performed.

The enthalpy of formation of a compound can be defined as the difference in total energy of the compound and the energies of its constituent elements in their stable states:

$$\Delta_f H = E_{\text{total}}^{Zr_xGe_{1-x}} - xE_{\text{total}}^{\text{Zr-hcp}} - (1-x)E_{\text{total}}^{\text{Ge-Diamond}} \quad (1)$$

where $E_{\text{total}}^{Zr_xGe_{1-x}}$ is the total energy of the compound Zr_xGe_{1-x}, and $E_{\text{total}}^{\text{Zr-hcp}}$ and $E_{\text{total}}^{\text{Ge-Diamond}}$ are the total energies of Zr and Ge in their stable structures, respectively. Since the influence of pressure on the condensed phases was ignored and the energy was calculated at 0 K without any entropic contributions, the calculated energy of formation was taken to be equivalent to the enthalpy of formation at 298 K. It should be mentioned that the enthalpy of formation of the compound Zr_5Ge_4 has also been calculated by Ponweiser et al. [21] using ab initio method. The ab initio method is not employed to calculate the enthalpy of formation for compounds Zr_3Ge and ZrGe, because the crystallographic positions of the atoms in these compounds are not determined.

Thermodynamic model

The Gibbs energy function ${}^0G_i^{\varphi}(T) = G_i^{\varphi}(T) - H_i^{\text{SER}}$ for the pure element i (i = Zr, Ge) is expressed as

$${}^0G_i^{\varphi}(T) = a + b\cdot T + c\cdot T + \ln T + d\cdot T^2 + e\cdot T^{-1} + f\cdot T^3 + g\cdot T^7 + h\cdot T^{-9} \quad (2)$$

where H_i^{SER} is the molar enthalpy of the element i at 298.15 K and 1 bar in its stable element reference (SER) state, and T is the absolute temperature. In the present modeling, the Gibbs energies as a function of temperature are taken from the SGTE compilation by Dinsdale [22].

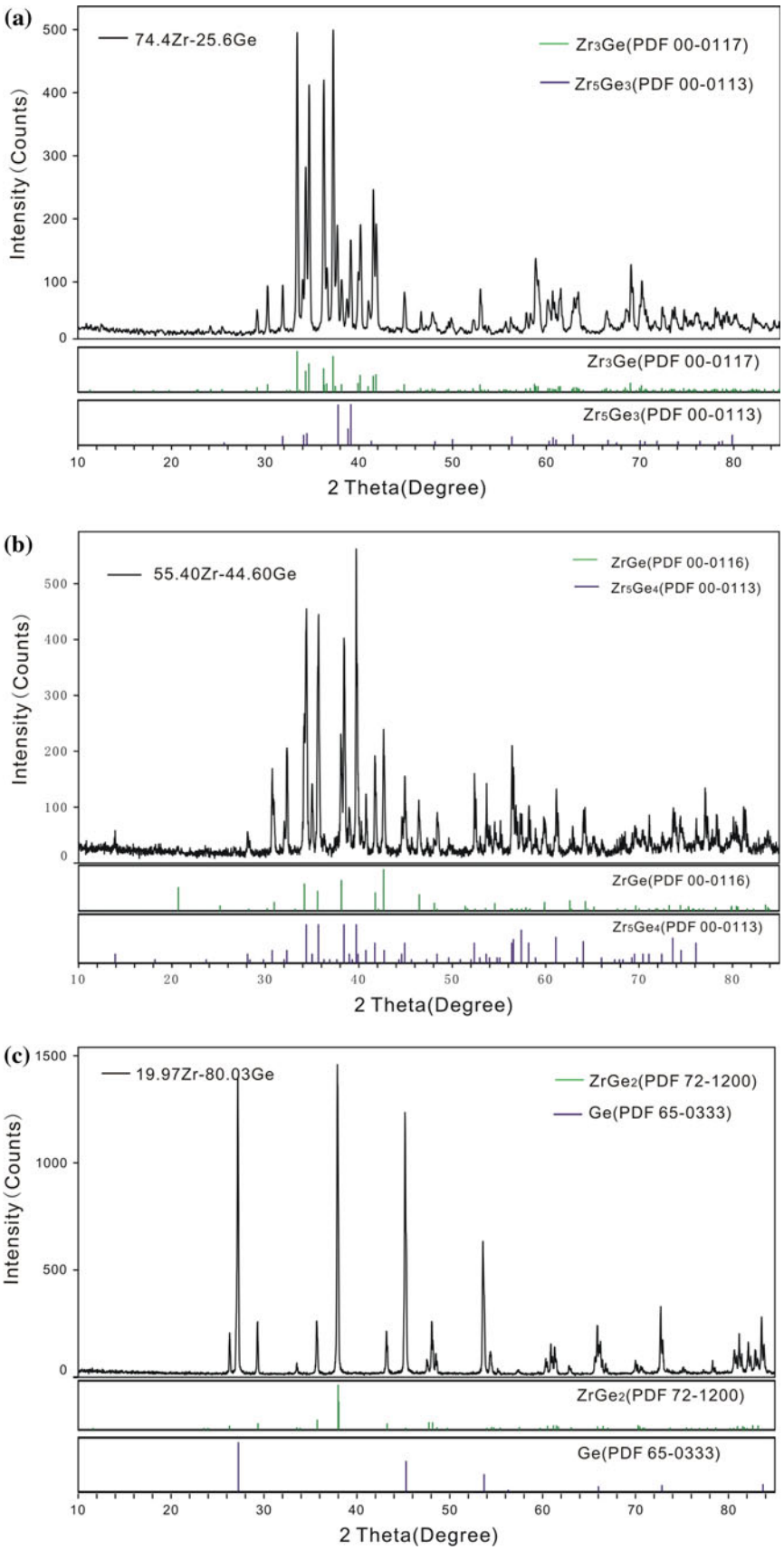

Fig. 3 The XRD patterns of alloy 1# (**a**), alloy 5# (**b**), and alloy 9# (**c**)

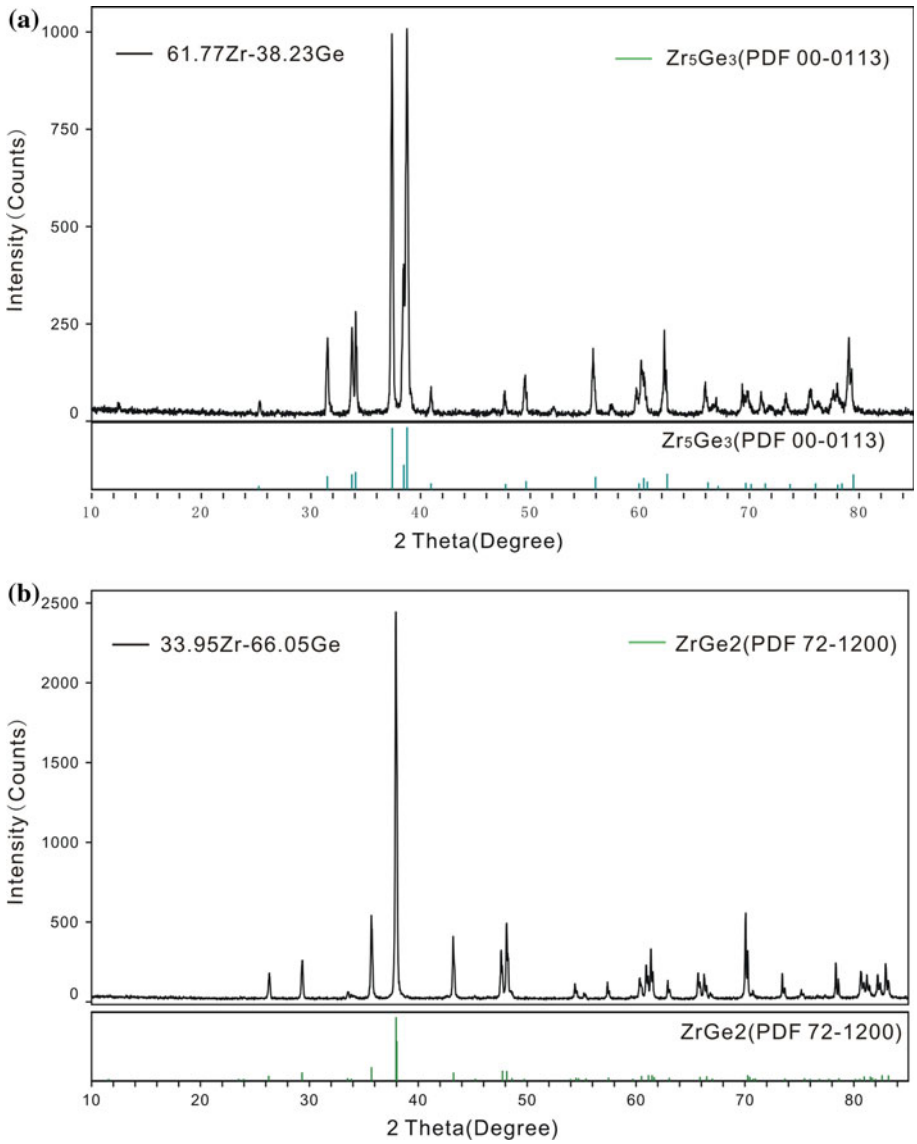

Fig. 4 The XRD patterns of alloy 3# (**a**) and alloy 8# (**b**)

The Gibbs energy for the solution phase (liquid (αZr) and (βZr)) is described by the Redlich–Kister polynomial [23]:

$$\begin{aligned} G_{\mathrm{m}}^{\mathrm{L}} - H^{\mathrm{SER}} &= (1-x)\cdot {}^{0}G_{\mathrm{Ge}}^{\mathrm{L}} + x\cdot {}^{0}G_{\mathrm{Zr}}^{\mathrm{L}} \\ &\quad + R\cdot T\cdot[(1-x)\cdot\ln(1-x) + x\cdot\ln x] \\ &\quad + x\cdot(1-x)[a_0 + b_0\cdot T + (1-2x)\cdot(a_1 + b_1\cdot T) + \cdots] \end{aligned} \tag{3}$$

in which H^{SER} denotes $(1-x)\cdot H_{\mathrm{Ge}}^{\mathrm{SER}} + x\cdot H_{\mathrm{Zr}}^{\mathrm{SER}}$, R is the gas constant, and x represents the mole fraction of Zr. The interaction coefficients a_j and b_j ($j = 0, 1, 2$) are to be evaluated in the optimization process.

In order to reduce the number of adjustable parameters, for the solution phases ((αZr) and (βZr)) the following approximate equation reported in Refs. [24] and [25] is adopted

$$14.0 * \Delta\bar{S}_{\mathrm{B}}^{\mathrm{Ex}} = \Delta\bar{H}_{\mathrm{B}} * \left(1/T_{\mathrm{m,A}} + 1/T_{\mathrm{m,B}}\right) \tag{4}$$

in which the relationship between the partial enthalpy $\Delta\overline{H}_{\mathrm{B}}$ and the partial excess entropy $\Delta\overline{S}_{\mathrm{B}}^{\mathrm{Ex}}$ depends on the melting points $T_{\mathrm{m,A}}$ and $T_{\mathrm{m,B}}$ of the components A and B. Consequently, for the solution phase ((αZr) and (βZr)) the a_0/b_0 in Eq. 3 is a constant. For the Ge–Zr system the constant is −10796.1.

The compounds Zr_3Ge, Zr_5Ge_3, Zr_5Ge_4, ZrGe, and $ZrGe_2$ are modeled as stoichiometric phases. The Gibbs energy is given by the following expression:

$$\begin{aligned} G\left(\mathrm{Zr}_x\mathrm{Ge}_y\right) - x\cdot H_{\mathrm{Zr}}^{\mathrm{SER}} - y\cdot H_{\mathrm{Ge}}^{\mathrm{SER}} \\ = x\cdot {}^{0}G_{\mathrm{Zr}}^{\mathrm{Hcp}} + y\cdot {}^{0}G_{\mathrm{Ge}}^{\mathrm{Diamond}} + \mathrm{A} + \mathrm{B}\cdot T \end{aligned} \tag{5}$$

where A and B are to be optimized.

Results and discussion

Detailed experimental results from XRD and SEM/EDX are presented in Table 3. The lattice parameters of identified phases were refined with the Jade.5 software [26]. Figure 1a, b shows the XRD patterns of alloys 4# and 7#, respectively. The corresponding backscattered electron images (BEI) are presented in Fig. 2a, b, respectively. The results of XRD and compositional analysis from EDX are in agreement. Both indicate that alloy 4# is located in a two-phase region of $Zr_5Ge_3 + Zr_5Ge_4$ and alloy 7# is located in a two-phase region of $ZrGe + ZrGe_2$.

Figure 3a–c shows the XRD patterns of alloys 1#, 5#, and 9#, respectively. The results of XRD show that alloys 1#, 5#, and 9# are located in the two-phase regions of $Zr_3Ge + Zr_5Ge_3$, $Zr_5Ge_4 + ZrGe$, and $ZrGe_2 + Ge$, respectively. Figure 4a, b shows the XRD patterns of alloys 3# and 8#, respectively. The results of XRD indicate that alloys 3# and 8# are located in the single-phase regions of Zr_5Ge_3 and $ZrGe_2$, respectively. The compositional analysis also confirmed the XRD results.

The XRD data confirmed all of the established Ge–Zr intermetallic phases and their crystal structures. The observed lattice parameters match closely those reported in Ref. [1]. The homogeneity regions for most of the Ge–Zr compounds are quite narrow. It should be mentioned that the composition of the Zr_5Ge_3 phase measured in this work is from about 37 to 40 at.% Ge. However, the experimental data about the homogeneity regions of Zr_5Ge_3 phase is limited. Consequently, in present work this phase is treated as a line compound.

The optimization of the thermodynamic parameters in the Ge–Zr system was performed with the PARROT module of the Thermo-calc software [27]. The step-by-step optimization procedure described by Du et al. [28] was adopted in the present assessment. In the optimization, each piece of experimental information is given a certain weight.

The optimization began with the liquid phase. First, the experimental enthalpy of mixing in the liquid phase in Ge-rich side was considered. Second, the intermetallic phases were considered in the optimization. In the case of the compounds, the compound Zr_5Ge_3 was taken into account first. Then other intermetallic phases were introduced in the modeling one by one. The first-principles computed enthalpy of formation for each compound was used as the good starting value for the parameter A in the present modeling. Parameters A and B were adjusted to describe the liquidus and invariant reactions. Then one regular parameter was employed for each of the (αZr) and (βZr) phases in order to account for the solubility data. Finally, the thermodynamic parameters of all the phases were optimized simultaneously based on all the reliable experimental data. The optimized thermodynamic parameters are listed in Table 4.

The computed Ge–Zr phase diagram using the present set of thermodynamic parameters is shown in Fig. 5. The calculated invariant equilibria are compared with the experimental ones in Table 5. It can be seen that the

Table 4 Summary of the thermodynamic parameters in the Ge–Zr system

Liquid: $(Ge,Zr)_1$
${}^0L^{liq}_{Ge,Zr} = -215873.63 + 28.39385 \cdot T$
${}^1L^{liq}_{Ge,Zr} = +38747.4 - 15.70641 \cdot T$
${}^2L^{liq}_{Ge,Zr} = +17000$
Bcc_A2: $(Zr,Ge)_1(Va)_3$
${}^0L^{bcc}_{Ge,Zr:Va} = -129330.87 + 12.03498 \cdot T$
Hcp_A3: $(Zr,Ge)_1(Va)_{0.5}$
${}^0L^{hcp}_{Ge,Zr:Va} = -185318.75 + 17.16534 \cdot T$
Zr_3Ge: $(Zr)_{3/4}(Ge)_{1/4}$
${}^0G^{Zr_3Ge}_{Zr:Ge} - 0.75 \cdot G^{hcp}_{Zr} - 0.25 \cdot G^{dia}_{Ge} = -54155.9 + 3.9848 \cdot T$
Zr_5Ge_3: $(Zr)_{5/8}(Ge)_{3/8}$
${}^0G^{Zr_5Ge_3}_{Zr:Ge} - 0.625 \cdot G^{hcp}_{Zr} - 0.375 \cdot G^{dia}_{Ge} = -73774.24 + 2.75 \cdot T$
Zr_5Ge_4: $(Zr)_{5/9}(Ge)_{4/9}$
${}^0G^{Zr_5Ge_4}_{Zr:Ge} - (5/9) \cdot G^{hcp}_{Zr} - (4/9) \cdot G^{dia}_{Ge} = -85535.45 + 5.91126 \cdot T$
ZrGe : $(Zr)_{1/2}(Ge)_{1/2}$
${}^0G^{ZrGe}_{Zr:Ge} - 0.5 \cdot G^{hcp}_{Zr} - 0.5 \cdot G^{dia}_{Ge} = -84427.18 + 4.80111 \cdot T$
$ZrGe_2$: $(Zr)_{1/3}(Ge)_{2/3}$
${}^0G^{ZrGe_2}_{Zr:Ge} - (1/3) \cdot G^{hcp}_{Zr} - (2/3) \cdot G^{dia}_{Ge} = -62260.8 + 1.78932 \cdot T$

In J mol-atoms^{-1}, temperature (T) in K

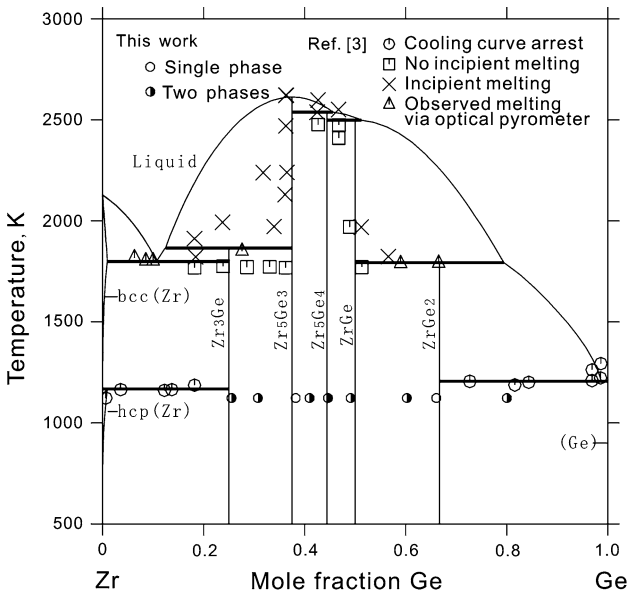

Fig. 5 Calculated Ge–Zr phase diagram along with the experimental data

Table 5 Presently calculated invariant reactions compared with those in the literature for the Ge–Zr binary system

Reaction	Type	Composition (at.% Ge)			T (K)	Reference
Liquid ⇔ (βZr) + Zr_3Ge	Eutectic	9.5	0.9	25	1810 ± 20	[3]
		10.68	0.936	25	1799	This work
(βZr) + Zr_3Ge ⇔ (αZr)	Peritectoid	~0	25	0.6–1.2	1169	[3]
		0.01	25	0.938	1169	This work
Liquid + Zr_5Ge_3 ⇔ Zr_3Ge	Peritectic	16–18	37.5	25	1860 ± 20	[3]
		12.44	37.5	25	1865	This work
Liquid ⇔ Zr_5Ge_3	Congruent	37.5	37.5		2603 ± 50	[3]
		37.5	37.5		2613	This work
Liquid + Zr_5Ge_3 ⇔ Zr_5Ge_4	Peritectic	45.61	37.5	44.44	2538	This work
Liquid + Zr_5Ge_4 ⇔ ZrGe	Peritectic				2513 ± 35	[3]
		51.21	44.44	50	2498	This work
Liquid + ZrGe ⇔ $ZrGe_2$	Peritectic				1793 ± 20	[3]
		79.45	50	66.67	1793	This work
Liquid ⇔ (Ge) + $ZrGe_2$	Eutectic	98.7	100	66.67	1207	[2]
		98.72	100	66.67	1207	This work

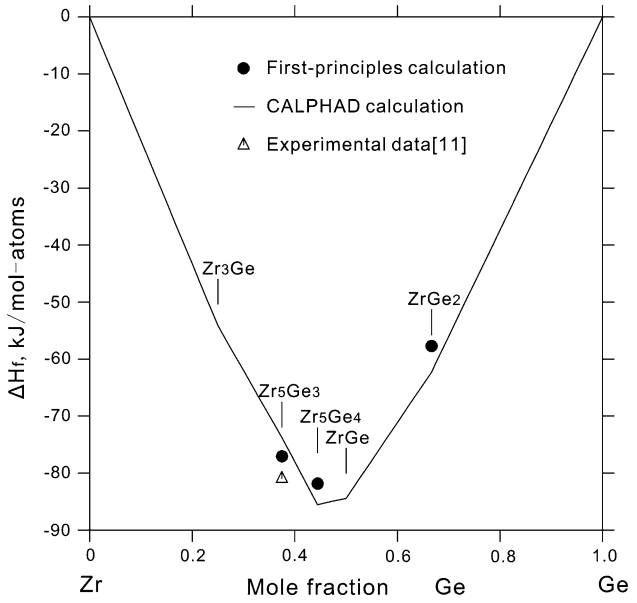

Fig. 6 Calculated enthalpies of formation at 298.15 K along with the first-principles calculation and the experimental data [11]

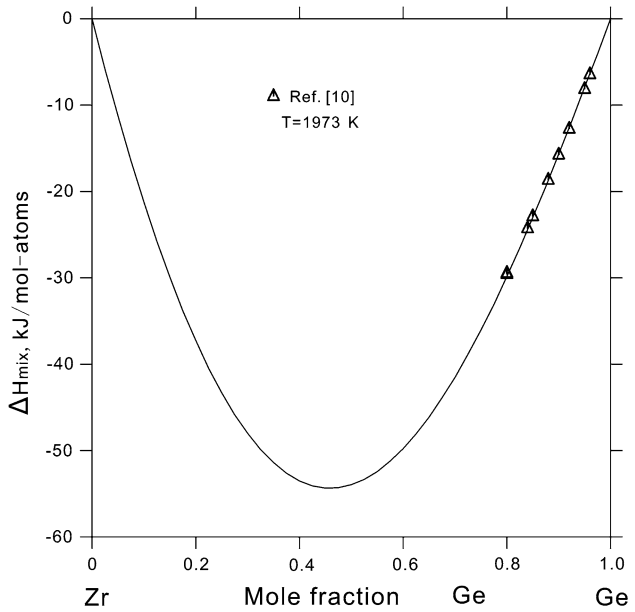

Fig. 7 Calculated enthalpies of mixing for liquid at 1973 K, compared with the experimental data [10]. The reference states are liquid Ge and liquid Zr

present modeling agrees well with the experimental data from Ref. [3]. The reaction temperatures of invariant reactions Liquid + Zr_5Ge_3 ⇔ Zr3Ge and Liquid ⇔ βZr + Zr3Ge reported in Ref. [3] are only 50-degree different, but the composition of the peritectic point is noticeably higher than the eutectic point. As a consequence it is difficult to model both reactions reasonably simultaneously. The peritectic point of Liquid + Zr_5Ge_3 ⇔ Zr3Ge according to at present modeling is 12.44 at.% Ge, the value is different from the experimental one at about 17 at.% Ge in Ref. [3].

Figure 6 presents the calculated enthalpies of formation from CALPHAD modeling compared with those from first-principles method and experimental data. The good agreement demonstrates that first-principles calculations can provide reliable values when the experimental data are not available.

Figure 7 presents the calculated partial enthalpies of mixing for liquid at 1973 K compared with the experimental data. It can be clearly seen that the calculation can satisfactorily account for these data.

Conclusions

- The phase diagram and thermodynamic data for the Ge–Zr system have been critically reviewed. Nine alloys were used to detect the phase stabilities of the compounds. It is found that the compounds exist in the stable phase diagram.
- An optimum set of thermodynamic parameters for the Ge–Zr system was obtained by considering the results of this work and critically assessed literature data. The calculated phase diagram and thermodynamic properties are in good agreement with the experimental data and first-principles calculation. A hybrid methodology of CALPHAD, first principles calculation and key experiment in the thermodynamic investigation is highly recommended.

Acknowledgements The financial support from the Creative Research Group of National Natural Science Foundation of China (Grant No. 50721003) and State Key Laboratory of Advanced Welding Production Technology, Harbin Institute of Technology of China is acknowledged.

References

1. Rudometkina MV, Seropegin D, Shvyryaeva EE (1988) J Less-Common Met 138:263
2. Abriata JP, Block JC, Arias D (1986) Bull Alloy Phase Diagr 7:43
3. Carlson ON, Armstrong PE, Wilhelm HA (1956) Trans ASM 48:843
4. Rossteutscher W, Schubert K (1965) Z Metallkd 56:813
5. Pfeifer HU, Schubert K (1966) Z Metallkd 57:884
6. Seropegin YuD, Bodak OI, Guseva IA, Penteleimonov LA (1980) Vestn Mosk Univ Ser 2 Khim 21((5):511
7. Zatorska GM, Pavlyuk VV, Davydov VM (2004) J Alloys Compd 367:80
8. Ponweiser N, Ipser H, Richter KW (2008) J Alloys Compd 452:80
9. Marker CJ, Effenberger HS, Richter KW (2009) Solid State Sci 11:1475
10. Beloborodova EA (1996) Powder Metall Met Ceram 35(Nos. 7–8):389
11. Jung WG, Kleppa OJ (1991) J Less-Common Met 169:93
12. Kohn W, Sham L (1965) Phys Rev A 140:1133
13. Perdew JP, Chevary JA, Vosko SH, Jackson KA, Pederson MR, Singh DJ, Fiolhais C (1992) Phys Rev B 46:6671
14. Blöchl PE (1795) Phys Rev B 50(1994):3
15. Kresse G, Furthmüller J (1996) Phys Rev B 54:11169
16. Kresse G, Furthmüller J (1996) Comput Mater Sci 6:15
17. Perdew JP, Burke K, Ernzerhof M (1996) Phys Rev Lett 77:3865
18. Monkhorst HJ, Pack JD (1976) Phys Rev B 13:5188
19. Methfessel M, Paxton AT (1989) Phys Rev B 40:3616
20. Blöchl PE, Jepsen O, Andersen OK (1994) Phys Rev B 49:16223
21. Ponweiser N, Warczok P, Lengauer CL, Richter KW (2009) Solid State Sci 11:395
22. Dinsdale AT (1991) Calphad 15:317
23. Redlich O, Kister AT (1948) Ind Eng Chem 40:345
24. Kubaschewski O (1981) High Temp High Press 13:435
25. Tanaka T, Gokcen NA, Morita Z (1990) Z Metallkd 81:349
26. JADE 5.0 (2001) Users guide for XRD pattern processing. Materials Data Inc., Livermore, CA, USA
27. Sundman B, Jansson B, Andersson JO (1985) Calphad 9:153
28. Du Y, Schmid-Fetzer R, Ohtani H (1997) Z Metallkd 88:545